Pharmaceutical Sciences and Drug Design
ISSN: 3062-4428
2026, Volume 6, Issue 1, Page No: 72-85

Available online at: www.galaxypub.co/page/journals

Galaxy Publication

Insights into Omeprazole Release from Solid Dosage Forms via Thermal and Kinetic Analysis

Daniel Fischer[1]*, Laura Meier[1], Thomas Braun[2], Stefan Koch[2], Felix Roth[1]

[1]Department of Drug Design and Pharmaceutical Innovation, Faculty of Pharmacy, University of Freiburg, Freiburg, Germany.
[2]Department of Molecular Therapeutics, Faculty of Engineering, Karlsruhe Institute of Technology, Karlsruhe, Germany.

***E-mail** ✉ daniel.fischer@outlook.com

Received: 29 October 2025; **Revised:** 08 February 2026; **Accepted:** 12 February 2026

ABSTRACT

The central aim pursued in this work was to investigate and assess the capacity of designated excipients to yield efficacious sustained-release omeprazole platforms. Toward this end, six distinct excipients were chosen (lactose monohydrate, medium-viscosity alginic acid, Avicel® PH-101, Avicel® PH-102, PVP K-30, and magnesium stearate). Selection was guided by criteria grounded in the physicochemical attributes of these materials (e.g., minimal toxicity) and their economic accessibility. Two excipient combinations were employed for tablet preparation, applying distinct methodologies characterized by practicality, modest expense (straightforward blending, compaction, and wet granulation), and limited time demands. The experimental outcomes revealed that the fabricated systems responded favorably, both in terms of tablet properties (hardness, dimensions, compositional uniformity) and in their ability to liberate omeprazole in a delayed fashion post-administration. Notably, one formulation (F7) exhibited a release pace comparable to that of the marketed product omeprazole Losec® (80% liberated within a two-hour window), whereas formulation F3 demonstrated a slower yet relatively consistent release extending over a longer span (no less than four hours) and may therefore be regarded as a promising foundation for the development of prolonged, stable-release delivery constructs (e.g., 24 h release) for pharmaceutical agents. The remaining preparations displayed analogous, intermediate-duration release profiles. Every release curve was additionally interpreted through the lens of interactions between excipients themselves and/or between excipients and OME, as probed via thermal analysis methodologies. In summation, the systems explored herein are characterized by comparatively low production costs, elevated performance, and a range of omeprazole release rates. Accordingly, they can be considered promising for future application with other active compounds, subject to suitable adjustments.

Keywords: Omeprazole, Excipients, Thermogravimetric analysis (TGA), Differential scanning calorimetry (DSC), Sustained release

How to Cite This Article: Fischer D, Meier L, Braun T, Koch S, Roth F. Insights into Omeprazole Release from Solid Dosage Forms via Thermal and Kinetic Analysis. Pharm Sci Drug Des. 2026;6(1):72-85. https://doi.org/10.51847/qUS0NdGLuG

Introduction

Bearing the molecular formula C17H19N3O3S and a mass of 345.42 g/mol, omeprazole (OME) constitutes a 5-methoxy-2-[(4-methoxy-3,5-dimethylpyridin-2-yl)methanesulfinyl]-1H-benzimidazole. Its architecture incorporates a substituted pyridine moiety, bridged to a substituted benzimidazole via a -CH2S(=O)- linker. Possessing tri-coordinated sulfonyl sulfur in a pyramidal arrangement, the molecule can manifest as an (R)- or (S)-enantiomer. That said, omeprazole exists as a racemic mixture; within the acidic interior of gastric parietal cells, both enantiomeric forms undergo conversion to achiral sulfenic acid and/or sulfenamide intermediates. These subsequently interact with H+/K+-ATPase, thereby blocking the acid-secreting function of parietal cells. Hence, from a therapeutic standpoint, it falls into the category of proton pump inhibitors (PPIs) [1-3]. Beyond this, OME is used to manage peptic ulcer disease (PUD), Zollinger–Ellison syndrome, and other conditions [2,

4]. PPIs are characterized as membrane-permeable weak bases, with pKa1 values between 3.8 and 4.9 [5-8]. Each PPI variant forms disulfide linkages with specific cysteine residues on ATPases. In omeprazole's case, the linkage sites are cysteines 813 and 822 [6]. The original synthesis of omeprazole dates to 1979, when it was labeled compound H168/68 by Astra AB, an entity now merged into AstraZeneca, and subsequently marketed under the brand Losec®. To avoid confusion with the established diuretic Lasix®, the US Food and Drug Administration (FDA) mandated that Prilosec® be renamed for that market [9, 10].

For an encapsulated pharmaceutical agent to become fully active and achieve its maximal therapeutic effect, it must escape the capsule shell and enter the systemic circulation. Two principal delivery platforms govern this process: the Immediate-Release Drug Delivery System (IRDDS) and the Modified-Release Drug Delivery System (MRDDS) [11, 12]. Formulations classified within the IRDDS category possess the ability to undergo rapid dissolution upon oral intake, consequently discharging the active ingredient without delay. This yields swift compound absorption and a prompt therapeutic onset [11-13]. Nonetheless, despite a range of advantages—spanning economic viability, substantial drug-loading capacity, adaptability in tablet manufacturing and packaging, and superior stability, bioavailability, and solubility of the medicinal formulation—this system falters when tasked with delivering agents formulated as prodrugs or those exhibiting lipophilic characteristics [12, 14]. For these two groupings, the Modified-Release System is judged to be a better fit.

In general, the designation Modified-Release Drug Delivery System covers pharmaceutical products that modulate the timing and/or rate of drug release. Such items are sorted into three overarching types: (1) extended-release preparations, (2) delayed-release preparations, and (3) targeted-release preparations [11, 12, 15]. With respect to these classifications, delayed release characterizes items wherein a distinct fraction or fractions of the drug are discharged at a juncture distinct from immediately post-dosing. However, an initial fraction may be released immediately. This strategy proves exceptionally valuable for drug types prone to inducing gastric mucosal irritation (e.g., NSAIDS), those highly vulnerable to swift decomposition within the diverse acids of the gastrointestinal tract, or those requiring availability in the lower intestinal segments to address localized disorders such as inflammatory bowel diseases. Moreover, delayed-release formulations are used when a significant lag is required between administration and the onset of the therapeutic response, as in individuals with rheumatic arthritis. Usually, this temporal offset is achieved by applying an enteric film to dosage forms such as tablets and capsules, thereby safeguarding the active ingredient from the harsh acidic environment of the mucosa and enabling its liberation in the comparatively neutral surroundings of the small intestine [11, 12, 15, 16].

As stated earlier, omeprazole, a representative of the proton-pump inhibitor class, is highly susceptible to rapid decomposition in the highly acidic gastric secretions characteristic of the upper gastrointestinal tract. For this reason, systemic absorption and subsequent activation necessitate that omeprazole avoid prompt release upon entry into the body or the stomach; rather, its release must be delayed until the formulation reaches the lower gastrointestinal tract (the small intestine), where a virtually neutral environment prevails (pH = 6.8). A range of delayed-release preparations accomplishes this feat, chiefly consisting of tablets and capsules encased in various gastroresistant coating materials [3, 4, 17, 18]. A particularly widespread coating agent is Eudragit®. The proprietary designation Eudragit® encompasses a broad family of highly thermoplastic copolymers based on polymethacrylate chemistry, available in anionic, cationic, and neutral configurations. Among these, the anionic variants are widely used in delayed-release delivery technologies, a status owed to their non-biodegradable, non-absorbable, and non-toxic profile, combined with dissolution behavior at pH levels above 6, which ensures the secure delivery of acid-labile therapeutic agents to the distal parts of the gastrointestinal tract [19-21].

Within the scope of the present work, omeprazole-bearing tablets incorporating suitable excipients were newly synthesized at a laboratory scale and subsequently enveloped in an Eudragit® layer. Their endurance in acidic buffer solution (pH 4.5) and dissolution rate under conditions simulating the small intestinal environment (pH 6.8) were then assessed. Outcomes were set alongside data from a widely marketed reference product with an analogous architecture and indication (Losec®), and a discussion of the respective strengths and weaknesses of the novel drug formats is presented. In addition, the release kinetic profiles of the varied dosage forms were analyzed, and interpretive explanations are offered here, resting upon excipient interaction data derived from thermogravimetric analysis (TGA) and differential scanning calorimetry (DSC) investigations.

Materials and Methods

Materials

Tablet and capsule manufacturing employed omeprazole pellets (Cipla Ltd., Mumbai, India), prepared in accordance with the British Pharmacopeia monograph and graciously supplied by Pharma Data SA (Lavrion, Greece). The pellet composition contained 8.5% w/w omeprazole, along with a mixture of excipients (Batch No. YXX4086, CIPLA). The additional excipients utilized comprised: No 0 hard gelatin capsules (Syndesmos, Athens, Greece), sodium alginate of medium viscosity (Alfa Aesar GmbH & Co KG, Schwerte, Germany), Avicel® PH-101 (Alfa Aesar GmbH & Co KG, Schwerte, Germany), Avicel® PH-102 (Sigma-Aldrich, Darmstadt, Germany), lactose monohydrate (Merck, Darmstadt, Germany), magnesium stearate (Riedel-De Haen, Seelze, Germany), and PVP K-30 (Sigma-Aldrich, Darmstadt, Germany). Every excipient conformed to pharmaceutical-grade specifications.

Buffer solutions for dissolution experiments were formulated using analytical-grade reagents (KH2PO4 and NaOH), both sourced from Sigma-Aldrich (Darmstadt, Germany).

The experimental setup made use of the following laboratory instrumentation: ATX224® high-precision analytical balance (Shimadzu, Kyoto, Japan), Turbula® T2F blender mixer (WAB, Nidderau, Germany), AR® 402 twin screw mixer (ERWEKA GmbH, Langen, Germany), Binder® F115 oven (Carbolite Gero GmbH & Co KG, Derbyshire, UK), AR® 400 cubic mixer (ERWEKA GmbH, Langen, Germany), IKA® RCT standard magnetic stirrer (LLG Labware, Meckenheim, Germany), 10 mm tableting die (Maassen GmbH, Möglingen, Germany), dry granulator (ERWEKA GmbH, Langen, Germany), THB 28 hardness tester (ERWEKA GmbH, Langen, Germany), PT-DT7 dissolution apparatus (Pharma Test, Hainburg, Germany), Multi 3410 Set 1 pH meter (Wissenschaftlich-Technische Werkstätten GmbH, Weilheim, Germany), MP 150 hydraulic press (Maasen GmbH, Möglingen, Germany), uniSPEC 2 UV-Vis Spectrophotometer (LLG Labware, Meckenheim, Germany), Titan3™ 0.45 μm regenerated cellulose syringe filters (Thermo Fisher Scientific Inc. Rockwood, TN, USA), and Q500IW Image Analysis system (Leica Microsystems, Wetzlar, Germany).

Methods

Granules' production

Lactose monohydrate and microcrystalline cellulose (Avicel® PH-101) were initially passed across a No. 20 mesh sieve before being mixed within a cubical mixer over 15 min. The blend was then introduced into the high-shear mixer granulator, where the binder solution (0.135% w/w PVP K30 in distilled water) was incorporated. The dampened mass obtained was spread onto furnace trays and held at 55 °C for 12 h. After drying, the granules were forced through a standard No. 12 sieve [22].

Formulation Production (capsule filling and tablet production)

An equal mass (235 mg) of omeprazole pellets was used throughout all formulations, and within formulations 2 through 7, a consistent amount (4.70 mg) of magnesium stearate was added. A conventional sieve was used to achieve homogeneous content by co-mixing the omeprazole pellets with the excipient during tablet formation. Moreover, the pellets exhibited excellent uniformity, a property indispensable for the ensuing stages of formulation development. The relative proportions of the remaining excipients for every formulation are detailed in the tabulated summary below **(Table 1).** The design logic behind the OME formulations centers on assessing how distinct excipient choices modulate interactions with the API, its dissolution behavior, and its liberation profile from the finished tablets.

Table 1. Composition of OME formulations.

Constituents (mg)	7 Tabs	6 Tabs	5 Tabs	4 Tabs	3 Tabs	2 Tabs	1 Caps
Omeprazole pellets (8.5% w/w) 1	235	235	235	235	235	235	235
Lactose monohydrate	143	-	117.5	117.5	117.5	235	-
Sodium alginate (medium viscosity)	-	-	-	-	117.5	-	-
MCC (Avicel® PH-102)	-	-	-	117.5	-	-	-
MCC (Avicel® PH-101)	85	-	117.5	-	-	-	-
Granules (36.3% Avicel® PH-101, 60.7% Lactose, 3% PVP K-30)	-	235	-	-	-	-	-
PVP K-30	7	-	-	-	-	-	-
Magnesium stearate	4.70	4.70	4.70	4.70	4.70	4.70	-

Total	474.70	474.70	474.70	474.70	474.70	474.70	235

1 granule composition.

Direct compression was used as the fabrication method for all formulations, except formulation F6, which was manufactured by wet granulation. In preparing the capsules (formulation 1), omeprazole was encapsulated within the gelatin shell. For every other formulation, the steps outlined next were performed; the solitary point of divergence pertained to formulation 6, wherein the three foundational excipients (Avicel® PH-101, lactose monohydrate, and PVP K-30) were subjected to dry granulation before incorporation.

First, the requisite excipient masses were determined using an ATX224® high-precision analytical balance and placed inside a small, sterile glass vessel. The vessel was then mounted in a Turbula® T2F blender mixer and blended for 10 min. Next, the omeprazole pellets were added to the excipient admixture, and blending continued for an additional 5 min. The omeprazole–excipient blend was then transferred to a 10 mm tableting die and compressed using an MP 150 hydraulic press. This sequence yielded homogenous tablets free from fissures or other apparent signs of mechanical weakness.

Tablet characterization (tablets' weight, thickness, and crushing strength uniformity)

Ahead of the dissolution trials, tablets from each of the formulations 2 through 7 were used to determine two fundamental physical properties (mass and dimensional specifications) per batch, along with hardness appraisal. An ATX224® high-precision analytical balance and a THB 28 hardness meter were deployed to quantify mass and crushing strength, respectively, whilst a vernier caliper captured geometric measurements (diameter and thickness).

Image analysis

Discrepancies in tablet attributes (including granule-based and physically mixed preparations) were assessed via image analysis. Image capture and manipulation were performed within a Leica Q500IW Image Analysis system, equipped with a JVCTK-C 1381 color camera and a Century Precision Optics C15838 (+7) lens for superior magnification. A fluorescent tube encircling the microscope glass served as the light source, with shielding to block extraneous ambient illumination.

Dissolution testing

Dissolution assessments for every formulation were undertaken on a PT-DT7 dissolution apparatus fitted with baskets (USP, 2007, Apparatus type I). A single standardized procedure was followed across all formulations, and the thermal conditions remained fixed at 37 ± 0.5 °C throughout the experimental timeframe. To commence, 3 capsules or tablets were individually placed in separate baskets and lowered into glass vessels prefilled with 900 mL of KH2PO4/NaOH buffer (pH 4.5). Sampling entailed drawing 5 mL of medium from each vessel at 15-minute intervals through the initial 45 minutes, with each withdrawal offset by replenishment using an identical volume of fresh buffer; absorbance readings were subsequently collected at 295 nm on a uniSPEC 2 UV-Vis Spectrophotometer. After the 45-minute interval, the baskets were transferred to vessels containing 900 mL of KH2PO4/NaOH buffer (pH 6.8). Solution aliquots were pulled every 15 minutes for a maximum duration of 285 minutes measured from the experiment's onset, and absorbance was determined at 301 nm.

Dissolution profile comparison

To compare the dissolution patterns of the test formulations and Losec®, plots of % omeprazole liberated over time were prepared. The t20%, t50%, and t90% metrics were also derived for each product, with tx% signifying the time point at which x% of the active constituent has been discharged from the dosage form.

Supplementing the tx% analysis, mean dissolution time (MDT) figures were computed through the expression detailed below (Eq. 1) [23]:

$$MDT = \frac{ABC}{W_{\infty}} \quad (1)$$

Where W∞ denotes the ultimate quantity of dissolved omeprazole, and ABC captures the region bounded by the drug dissolution plot and its limiting asymptote.

Data analysis

To identify and compare dissolution test kinetics, the in vitro release datasets for each formulation were fitted to the zero-order, first-order, Higuchi square root, and Korsmeyer–Peppas mathematical models.

Model-independent analysis of dissolution profiles

A model-independent profiling of dissolution behaviors across formulations was achieved by calculating both the difference factor (f1) and the similarity factor (f2). The f1 statistic captures the averaged relative divergence between a pair of curves evaluated at all recorded time points and obeys the following formulation (Eq. 2) [24]:

$$f_1 = \left\{\frac{[\sum_{t=1}^{n} | R_t - T_t |]}{\sum_{t=1}^{n} R_t}\right\} \times 100 \quad (2)$$

Where Rt reflects the mean percentage of the reference product dissolved at a given post-initiation time t, Tt reflects the mean percentage of the test product dissolved at that same post-initiation time t, and n equals the total count of temporal sampling points.

In contrast to f1, the f2 statistic is used to compare cumulative percentage dissolution trajectories for two samples. Its computation follows the equation laid out here (Eq. 3) [24]:

$$f_2 = 50 \times \log\left\{\left[1 + \frac{1}{n}\sum_{t=1}^{n}(R_t - T_t)^2\right]^{-0.5} \times 100\right\} \quad (3)$$

Where, mirroring the parameters in f1, Rt stands for the mean percentage of reference drug dissolved at post-initiation time t, Tt stands for the mean percentage of test drug dissolved at post-initiation time t, and n is the total count of temporal sampling points.

The f2 metric ranges from 0 to 100. As the mismatch between test and reference release profiles grows more pronounced, the f2 figure shrinks, inching closer to zero. Conversely, an f2 reading of 100 reflects a perfect overlap of the two curves. Under conventional interpretive guidelines, two dissolution profiles are accepted as comparable when $0 < f1 < 15$ and $50 \leq f2 < 100$.

Thermal analysis techniques

Thermogravimetric analysis (TGA) was run on a TGA 55 Thermogravimetric Analyzer (TA Instruments, New Castle, DE, USA). The temperature was elevated at 10 °C/min from ambient (26 °C) up to 600 °C, all under a nitrogen atmosphere flowing at 25 mL/min.

Differential scanning calorimetry (DSC) was performed using a DSC 25 (TA Instruments, New Castle, DE, USA). Specimens weighing 7–8 mg were crimped into aluminum pans and heated from 40 to 240 °C at a uniform ramp rate of 10 °C/min, with nitrogen purging at 50 mL/min.

Results and Discussion

Release kinetics of OME from different formulations

The data in **Table 2** confirm that all tablets resided within the acceptable boundaries for each tested parameter (mass, thickness, and fracture force), in line with established international norms [25]. **Figure 1** compares the image analysis of two OME formulations built from identical ingredients; F6 was manufactured by wet granulation, whereas F7 was manufactured by direct compression. The pellet sizes proved consistent, as portrayed and quantified in **Figure 2**. Given the pellet dimensions and the processing routes applied, the pellet distribution was fairly homogeneous. Even so, we cannot claim that our pellets reached a high level of uniformity. Crucially, it must be highlighted that tableting succeeded in every instance without any observable surface imperfections—specifically, capping or lamination phenomena were absent. The final tablet geometry remained stable both immediately after compaction and throughout the storage interval.

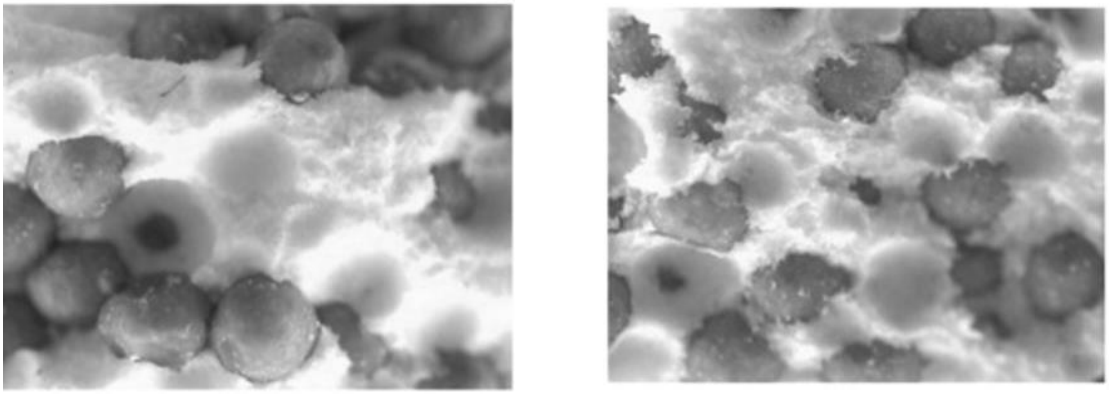

a) b)

Figure 1. Image analysis results from formulations F6 (a) and F7 (b); scale-magnification ×50.

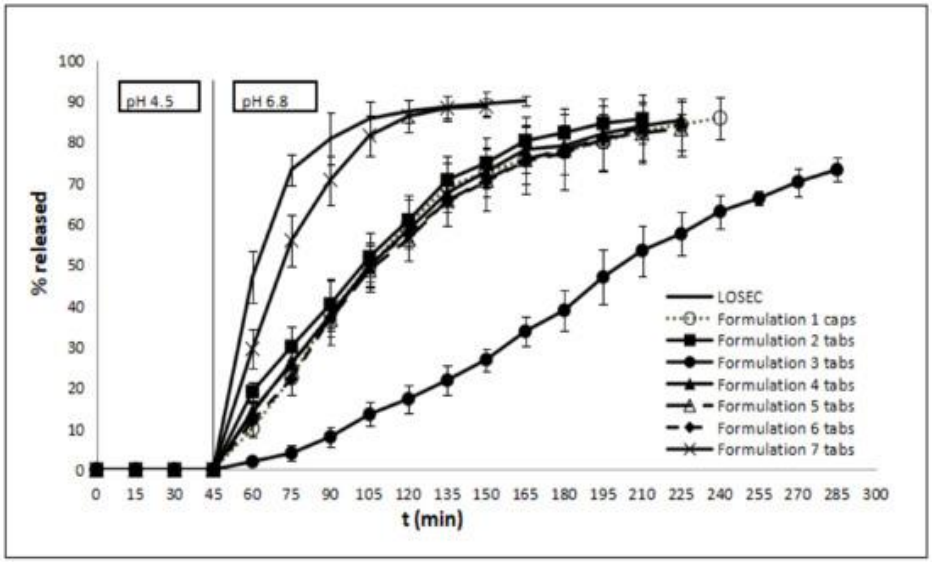

Figure 2. % Omeprazole release (mean ± SD) (n = 3) vs. time (min) for Losec® and formulations 1–7 (pH 4.5 for 45 min and pH 6.8 thereafter).

Table 2. Results of tablets' weight, thickness, and crushing strength uniformity.

Formulation code	Fracture resistance (N)	Average tablet thickness (mm) (± SD)	Mass (mg) (± SD)	Diameter (mm)
F2	50	4.3 ± 0.00	475.2 ± 1.3	10
F3	55	4.3 ± 0.00	474.3 ± 1.1	10
F4	53	4.3 ± 0.00	475.5 ± 0.8	10
F5	51	4.3 ± 0.00	475.2 ± 1.2	10
F6	81	4.3 ± 0.00	474.7 ± 1.9	10
F7	62	4.3 ± 0.00	475.1 ± 1.3	10

The dissolution traces for Losec® and the manufactured formulations are presented in **Figure 2**. A summary of the dissolution experimental findings is organized across **Tables 3-5**. Specifically, **Table 3** records the t20%, t50%, t90%, and MDT values for every formulation. To unravel the kinetic characteristics, the in vitro release data from the formulations were correlated with zero-order, first-order, Higuchi square root, and Korsmeyer–Peppas kinetic models **(Table 4)**.

Table 3. Kinetic release properties of the OME formulations.

Formulation	MDT	$t_{90\%}$	$t_{50\%}$	$t_{20\%}$
Losec®	64.96	165	62	52
F1	93.73	*	105	72

F2	89.89	*	102	62
F3	112.59	*	202	129
F4	92.41	*	105	72
F5	92.33	*	108	68
F6	93.11	*	105	72
F7	72.48	155	72	55

OME did not reach 90% release.

Table 4. R^2, release rate constants, and n values of the OME formulations.

Formulation	Korsmeyer-Peppas			Higuchi		First order			Zero order		
	R^2	K_{KP}	n	R^2	K_H	R^2	Y_1	K_1	R^2	Y_0	K_0
Losec®	0.86	1.25	0.92	0.57	7.85	0.46	55.17	−0.003	0.51	46.71	0.32
F1	0.87	1.40	0.77	0.76	5.21	0.78	26.21	−0.005	0.88	5.58	0.37
F2	0.93	0.64	0.93	0.75	5.57	0.84	24.37	−0.006	0.93	0.74	0.45
F3	0.98	0.01	1.76	0.57	3.15	0.92	7.58	−0.008	0.99	−22.25	0.35
F4	0.91	0.63	0.93	0.74	5.39	0.80	24.42	−0.006	0.90	0.66	0.43
F5	0.91	0.61	0.93	0.74	5.27	0.81	23.78	−0.006	0.91	0.52	0.42
F6	0.91	0.35	1.04	0.69	5.21	0.82	20.43	−0.007	0.92	−6.17	0.47
F7	0.85	1.63	0.82	0.73	7.21	0.76	32.32	−0.007	0.83	10.12	0.59

Table 5. f1 and f2 index.

Formulation	f_2	f_1
Losec® vs. 7	56.06	18.93
1 vs. 2	69.75	6.22
1 vs. 4	84.48	2.85
1 vs. 5	82.22	3.28
1 vs. 6	87.85	2.32
2 vs. 4	78.29	4.77
2 vs. 5	71.53	7.15
2 vs. 6	68.55	7.80
4 vs. 5	89.59	2.68
4 vs. 6	84.99	3.00
5 vs. 6	88.79	2.00

Drawing from **Figure 1**, one can observe that all formulations completely suppressed drug release at pH 4.5, indicating that the compaction forces exerted during tableting left the omeprazole pellets and their coating unharmed. The proportions of the selected excipients for pellet formulation were also appropriate to preserve pellet wholeness and medicinal content. With respect to Losec®, the commercial product, the active compound is rapidly released once the environment shifts to pH 6.8, reaching a plateau within 2 hours. The release pattern yielded by formulation F7 can be placed alongside that of Losec® (note the matching kinetic release parameters in **Table 3** as well as the f1 and f2 indices detailed in **Table 4**). In parallel, formulation F1 (capsules housing OME pellets) and F2 (tablets formed from a lactose monohydrate–OME pellet admixture) likewise exhibit closely aligned drug liberation data (note the matching kinetic release parameters in **Table 3** and the f1 and f2 indices in **Table 4**). Standing apart, formulation F3, formulated with sodium alginate, exhibits a considerably more drawn-out release profile compared with the remaining preparations. The interchange of Avicel® PH-101 with Avicel® PH-102 (as reflected in formulations F5 and F4, respectively) revealed no meaningful differences in drug release performance. Comparing F6 and F7, which rely on an identical excipient panel, F6 incorporates those excipients alongside OME pellets in a granulated state. At the same time, F7 introduces them purely as powders—a distinction that one might conjecture could promote a somewhat quicker release onset. Based on the dissolution results, every formulation eventually released the entire encapsulated active agent. For this reason, none of the fabricated formulations suffered from drug content inhomogeneity.

It can therefore be reasoned that formulations F1, F2, F4, F5, and F6 share essentially superimposable drug release signatures, implying that the pellets themselves govern the liberation process rather than the ancillary excipients

distributed within the tablet matrices, which presumably operate as simple bulking materials. Such a scenario is hardly unexpected, given that the excipients are basic fillers lacking specialized functional attributes. Once the Eudragit coat dissolves, the tablets break apart relatively quickly (at a rate dependent on their individual hardness).

Thermotropic behavior of OME formulations

The thermal behavior of OME has attracted considerable attention within the published literature [26-28]. In our investigation, emphasis was placed on the thermal response and robustness of omeprazole under conditions in which none of the fabrication stages introduced thermal manipulation of the API. This choice was informed by the well-documented notion that compression processes modify the thermotropic fingerprints of active compounds through molecular-level interactions among formulation ingredients and the mechanical stresses inherent to tablet or granule production. Furthermore, establishing the thermal benchmark of pristine omeprazole holds considerable value for comparative evaluation. Prior studies have sought to determine the most stable form of OME across diverse physical presentations (granules versus loose powders), temperature ranges, and acidity levels employing DSC. TGA work further demonstrated that degradation sets in at 135 °C and that both the heating rate and the eutectic character of thermal breakdown products influence the process, causing a progressive depression of omeprazole's melting point under incremental temperature elevation [26-28]. The present study set out to characterize the thermal endurance and response of OME distributed among varying formulations via TGA and DSC, respectively. Corresponding analyses of the excipient blends were likewise undertaken using the same instrumental techniques for benchmarking purposes. DSC and TGA results acquired for the pellets appear within **Figure 1** (corresponding to F1). Given that F1 represents OME pellets enclosed in capsules, the thermal analyses were directly conducted on the encapsulated contents—i.e., the pellets.

Turning to the TGA data **(Figure 3),** all excipient formulations exhibited an early degradation phase that initiated at roughly 139 °C, which can be assigned to the expulsion of moisture from the excipient admixtures. This was trailed by the principal breakdown stage commencing near 199 °C for LMSA and roughly 219 °C for the remaining excipient blends. Regarding LMSA, the decomposition process terminated at 249 °C. The incorporation of Avicel® PH-101 or Avicel® PH-102 shifted the completion of degradation to 338 °C and 339 °C, respectively. Conversely, the inclusion of PVP extended the final decomposition boundary to 343 °C. This central degradation step is tied to the release of water molecules retained in the excipient formulations. The primary factor distinguishing Avicel® PH-101 from Avicel® PH-102—both falling under the microcrystalline cellulose umbrella—is the extent of particle clustering, which is more pronounced in the latter [29]. Owing to this, no noteworthy differences were registered at the ultimate stage of the decomposition trajectory.

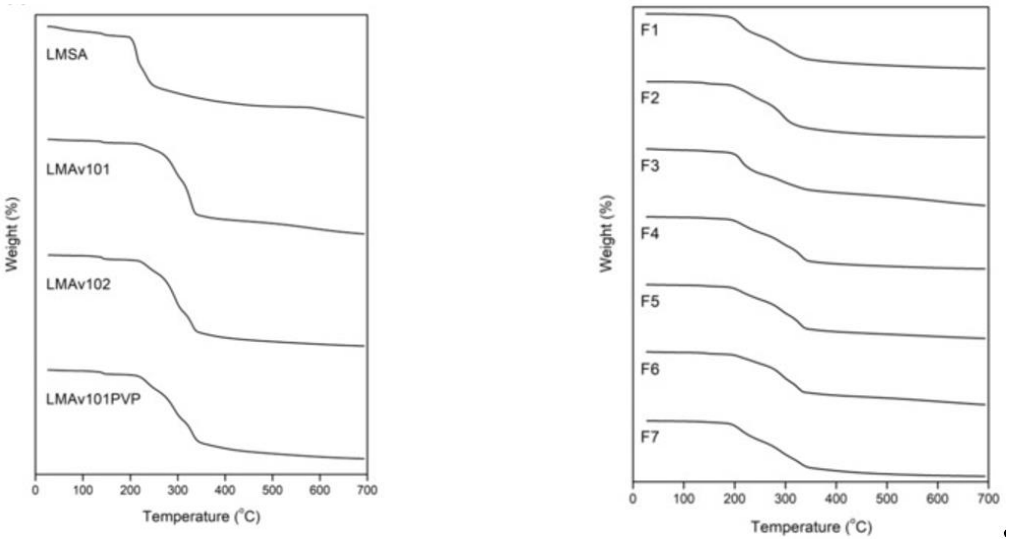

a) b)

Figure 3. TGA curves of (a) excipients and (b) formulations of OME (LMSA: lactose monohydrate/sodium alginate; LMAv101: lactose monohydrate/Avicel 101; LMAv102: lactose monohydrate/Avicel 102; LMAv101PVP: granules).

Regarding the OME preparations, the capsule form showed a notably different decomposition pathway compared to the other dosage forms. To elaborate, F1 underwent breakdown commencing at 190 °C and concluding at 336 °C, without any discernible dehydration stage. In contrast, formulations F2 through F7 exhibited primary decomposition onset between 191 and 196 °C, preceded by an early phase at 138–140 °C, ascribed to the previously discussed dehydration step.

Among the compressed tablet formulations, the temperature range over which degradation occurred proved markedly dependent on the excipients used. In the case of F2, which relies exclusively on lactose monohydrate, the principal decomposition reached completion at 323 °C. By comparison, the addition of sodium alginate, Avicel® PH-101, or Avicel® PH-102 prolonged the endpoint by roughly 20 °C **(Figure 3b).**

Consistent with our previously published findings, sodium alginate exhibits a distinctive endothermic band spanning 120–190 °C, with a midpoint around 163 °C [30]. Concurrently, lactose monohydrate exhibits two signature endotherms at 147 °C and 210 °C **(Figure 4a)**. When these two materials were combined, an endothermic signal emerged near 150 °C, shifted closer to the characteristic transition of lactose monohydrate—an observation we attribute to the interplay of simultaneous thermal events from both components. In our interpretation, these observations are intimately connected to the dehydration phenomenon affecting sodium alginate and the hydrophilic functional groups arrayed along its polymeric chain [31, 32]. Stated another way, the blended excipients exhibited a cooperative superimposition of the thermal signatures of each ingredient, manifesting as a broad endotherm extending up to 140 °C, derived from sodium alginate dehydration, immediately followed by a sharp endothermic peak centered around 150 °C, which aligns with the diagnostic dehydration signal of lactose monohydrate.

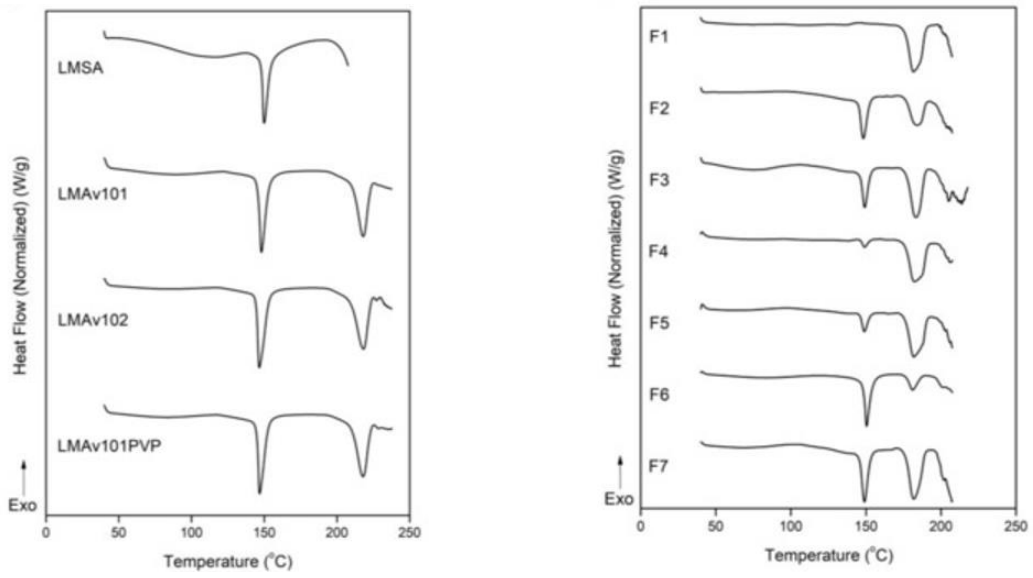

a) b)

Figure 4. DSC curves of (a) excipients and (b) formulations of OME (LMSA: lactose monohydrate/sodium alginate; LMAv101: lactose monohydrate/Avicel 101; LMAv102: lactose monohydrate/Avicel 102; LMAv101PVP: granules).

The characteristic endothermic feature of lactose monohydrate remains essentially unchanged in the company of other excipients, yet the melting enthalpy is augmented **(Figure 4a; Table 6).** The addition of either Avicel® PH-101 or Avicel® PH-102 promotes the development of a new endothermic signal located at 218 °C **(Figure 4a).** The enthalpy magnitude recorded for the 218 °C peak is greater for Avicel® PH-102 than for Avicel® PH-101, suggesting that the more extensively agglomerated state requires a larger energy input to undergo melting **(Figure 4a; Table 6).**

Table 6. DSC calorimetric values of excipients and formulations of OME.

Sample	ΔH_2 (J/g)	T_2 (°C)	ΔH_1 (J/g)	T_1 (°C)
LMSA	-	-	49.4	150.0

LMAv101	57.7	218.0	57.1	148.0
LMAv102	83.9	218.2	77.3	146.6
LMAv101PVP	78.9	217.9	71.2	146.8
F1	65.2	181.6	-	-
F2	34.9	183.7	27.8	148.3
F3	33.5	183.2	13.5	149.2
F4	52.5	182.3	3.8	149.1
F5	45.1	181.8	8.5	148.9
F6	19.4	181.0	49.7	150.4
F7	39.0	181.8	21.3	149.0

With the sole exception of F1, every formulation yielded an endothermic transition falling between 148.3 °C and 150.4 °C. The enthalpy associated with this transition varied substantially across formulations **(Figure 4b; Table 6)**. Beyond this, a second endothermic event was observed across all formulations near 180 °C, with negligible enthalpy variation across the set **(Figure 4b; Table 6)**. These observations are further explored in the subsequent section, yielding an interpretation that sheds light on OME's release behavior.

The multi-unit pellet tablet, in which coated pellets serve as the vehicle for modified drug delivery, is an effective therapeutic alternative to immediate-release dosage forms. Three primary advantages include ease of ingestion, the ability to subdivide without compromising the release behavior of individual units, and a predictable dispersal pattern of the multiparticulates along the gastrointestinal tract. From a manufacturing standpoint, multi-unit pellet system tablets can be fabricated at a substantially lower cost than pellet-filled capsules, given the considerably higher tableting throughput. Notwithstanding these benefits, production-related hurdles—such as compromised pellet integrity and content nonuniformity—have historically hindered their broader adoption [33-35].

Several excipients were required to facilitate compaction and protect the pellet coating from damage throughout the tableting sequence. As noted earlier, the optimal materials for pellet tableting should prevent pellet-to-pellet contact, thereby acting as a protective buffer during compression [36, 37]. It has been reported that 29% of the excipient is necessary to occupy the void spaces among tightly packed spheres. Yet, tablet variations remain acceptable at pellet loadings approaching approximately 50%, even when using non-granulated excipients [37]. In the present case, nearly 50% excipient content was employed to generate a separating layer between coated pellets, preventing adhesion and yielding mechanically robust tablets at modest compression pressures, all while exerting either negligible or, in certain instances, some influence on drug liberation. The excellent cooperativity among our excipients is further corroborated by DSC investigations performed on both the neat excipient blends and the OME-loaded formulations **(Figure 4; Table 6)**. Cooperativity, a thermal parameter that reflects the degree of uniformity of a transition and is quantified as half the width at half the peak height, is relevant here. This thermal index bears a direct relationship to compaction performance, since the formulation process hinges critically on intermolecular interactions between the various constituents. Beyond their compaction-related role, the excipients also had to ensure a homogenous pellet–excipient blend, circumventing segregation and the associated tablet weight variability; toward this end, coarser granules were additionally trialed for comparative assessment.

Sodium alginate is a linear, hydrophilic, colloidal polyuronic acid composed of guluronic and mannuronic acid residues, capable of forming gels with differing architectures at acidic versus neutral pH. At low pH (pH = 3), hydrogen bonding forms among the sodium alginate strands, swiftly transforming the material into alginic acid, which swells and becomes insoluble. Under these circumstances, drug release is entirely governed by diffusion through the polymer network. By contrast, at neutral pH, the alginic acid strands form a gel matrix via cross-links formed between their carboxyl groups and assorted cations, notably calcium ions. The selectivity with which alginic acid associates with various cations scales with the fraction of guluronic acid monomers present in the polymer. It has been shown that a higher guluronic acid content results in stronger cation binding and, correspondingly, enhanced mechanical rigidity of the resultant gel [38-45]. Hence, the emergence of a viscous gel phase exerted a pronounced effect on drug liberation, extending the OME release duration at neutral pH, as evidenced in F3.

Microcrystalline cellulose (MCC) ranks among the ubiquitous pharmaceutical excipients, functioning as a binding agent, disintegrant, bulking material, and anti-adherent. The two most prevalent grades are Avicel® PH-101 and Avicel® PH-102; the former has a nominal average particle size of 50 μm and is typically used in wet granulation

workflows, while the latter has a nominal average particle size of 100 µm and is used in direct compression processes [46]. Avicel® PH-101 represents the archetypal MCC grade, whereas Avicel® PH-102 corresponds to a partially agglomerated variant exhibiting a broader particle size span and marginally improved flow characteristics. Both grades displayed largely analogous thermotropic signatures, as evidenced by TGA and DSC analyses **(Figures 3 and 4; Table 6)**. Investigators who have examined their disparities in packing and flow behavior attributed these differences to variations in moisture levels, particle morphology, and granulometric spread. At the same time, neither grade manifests a meaningful divergence in compressibility [29, 47]. Within the confines of the present study, swapping Avicel® PH-101 for Avicel® PH-102 (formulations F5 and F4, respectively) failed to yield any notable shift in drug release. In our assessment, such findings are closely tied to the equivalent interactions that both grades have with the remaining excipients and OME, a conclusion supported by the DSC data **(Table 6)** [48].

Polyvinylpyrrolidone (PVP), also referred to as polyvidone or povidone, is a biodegradable, water-soluble polymer synthesized from its monomeric building block, N-vinylpyrrolidone. Beyond its hydrophilic character, PVP boasts outstanding dissolution capacity across solvents of widely differing polarities and dependable binding attributes. The aqueous solubility of the PVP K-30 grade (35,000–51,000 Daltons) selected for this work contributed favorably to drug dissolution behavior. Moreover, its viscosity exerted a considerable influence on the liberation of the poorly water-soluble drug OME [49, 50]. Specifically, the low-viscosity gel that formed during tablet dissolution facilitated the required suspension of OME within the polymeric network, thereby accounting for the accelerated release rate observed in formulation F7.

Both the wet granulation and direct compression routes proved suitable for fabricating OME tablet compositions. Consistent with published accounts, the granulated material exhibited superior flow, compressibility, and compactability compared with the directly compressed formulation [51]. It is recognized that wet granulation tends to yield tablets of greater hardness than those produced via direct compression, as tablet hardness depends on compaction force and granule or crystal resilience [51]. The formation of liquid bridges, followed by their crystallization and the hardening of the binding agents through drying, can also account for the elevated hardness values typical of wet-granulated compacts [52]. Owing to these factors, the granulation-based formulation (F6) exhibited a more sustained liberation profile than its directly compressed counterpart (F7). Moreover, the secondary endothermic transition in F7 demands a larger energy input for melting, which could potentially ease OME liberation from F7 relative to F6 **(Figure 4)**, considering that dissolution velocity and drug discharge are phenomena intimately linked to the melting points of excipients and the intermolecular interplay between excipients and APIs [53].

Furthermore, in addition to the generation of mechanically stronger granules, the particle size distribution differs significantly from that of the untreated excipients, yielding differing tablet hardness values. We supplied individual tablet hardness measurements, and those belonging to F6 and F7 are markedly distinct, separated by a 20 N gap. In our view, this observation is closely tied to the hardness profiles of these formulations and additionally influences the OME release trajectory. As indicated earlier, all formulations were prepared by direct compression, except F6, which was prepared by wet granulation. The divergent manufacturing pathways may also exert a decisive influence on the interactions among excipients and OME and/or among the excipients themselves, as they modify the thermal background of the employed materials. Finally, this thermal background, together with the presence of the granulating liquid during the wet granulation procedure, could be held responsible for the OME release behavior observed in the dissolution studies, as the literature suggests [53-55].

Conclusion

The experimental outcomes revealed that the fabricated systems responded favorably, both in terms of tablet properties (hardness, dimensions, compositional uniformity) and in their ability to liberate omeprazole in a delayed fashion post-administration. Notably, one formulation (F7) exhibited a release pace comparable to that of the marketed product omeprazole Losec® (80% liberated within a two-hour window), whereas formulation F3 demonstrated a slower yet relatively consistent release extending over a longer span (no less than four hours) and may therefore be regarded as a promising foundation for the development of prolonged, stable-release delivery constructs (e.g., 24 h release) for pharmaceutical agents. The remaining preparations displayed analogous, intermediate-duration release profiles. Every release curve was additionally interpreted through the lens of interactions between excipients themselves and/or between excipients and OME, as probed via thermal analysis

methodologies. In summation, the systems explored herein are characterized by comparatively low production costs, elevated performance, and a range of omeprazole release rates. Accordingly, they can be considered promising for future application with other active compounds, subject to suitable adjustments. The deployment of thermal analysis techniques is critical for probing interactions among formulation constituents and is instrumental for furnishing mechanistic rationales for the release profiles of encapsulated APIs.

Acknowledgments: The authors wish to thank Vassilios Roussis for providing the facilities for the TGA and DSC measurements. The authors would also like to thank Pharmadata S.A. for providing us with omeprazole beads for this investigation.

Conflict of Interest: None

Financial Support: None

Ethics Statement: None

References

1. Brandstrom A, Lindberg P, Junggren U. Structure-activity relationships of substituted benzimidazoles. Scand J Gastroenterol Suppl. 1985;108:15-22.
2. Massoomi F, Savage J, Destache CJ. Omeprazole: a comprehensive review. Pharmacotherapy. 1993;13:46-59.
3. Filho VJT, Andreazza IF, Sato MEO, Murakami FS. Development of a multiparticulate system containing enteric release mini-tablets of omeprazole. Braz J Pharm Sci. 2014;50:505-11.
4. El-Sayed A, Boraie NA, Ismail FA, El-Khordagui LK, Khalil SA. Assessment of the pharmaceutical quality of omeprazole capsule brands marketed in Egypt. East Mediterr Health J. 2007;13:1427-37.
5. Sachs G, Shin JM, Howden CW. Review article: the clinical pharmacology of proton pump inhibitors. Aliment Pharmacol Ther. 2006;23 Suppl 2:2-8.
6. Shin JM, Sachs G. Pharmacology of proton pump inhibitors. Curr Gastroenterol Rep. 2008;10:528-34.
7. Strand DS, Kim D, Peura DA. 25 years of proton pump inhibitors: a comprehensive review. Gut Liver. 2017;11:27-37.
8. El-Rouby N, Lima JJ, Johnson JA. Proton pump inhibitors: from CYP2C19 pharmacogenetics to precision medicine. Expert Opin Drug Metab Toxicol. 2018;14:447-60.
9. Farley D. Making it easier to read prescriptions. FDA Consum. 1995;29:25-7.
10. Lundell L. The physiological background behind and course of development of the first proton pump inhibitor. Scand J Gastroenterol. 2015;50:680-4.
11. Perrie Y, Rades T. FASTtrack: Pharmaceutics—Drug Delivery and Targeting. 2nd ed. London: Pharmaceutical Press; 2012. p. 1-24.
12. Shargel L, Wu-Pong S, Yu ABC. Applied Biopharmaceutics & Pharmacokinetics. 6th ed. New York: McGraw-Hill Education; 2012.
13. Saha S. Immediate release drug delivery systems: a current update. J Appl Pharm Res. 2018;6:1-9.
14. Nyol S, Gupta MM. Immediate drug release dosage form: a review. J Drug Deliv Ther. 2013;3:155-61.
15. Trenfield SJ, Basit AW. Nanotechnology for Oral Drug Delivery: From Concept to Applications. 1st ed. Amsterdam: Elsevier; 2020. p. 177-97.
16. Montero Mirabet M, Skalsky B. Advanced approaches for delayed-release formulations. ONdrugDelivery Mag. 2017;77:4-9.
17. Chakravarthy KK, Younus M, Shaik S, Pisipati SVV. Formulation and evaluation of enteric coated pellets of omeprazole. Int J Drug Dev Res. 2012;4:257-64.
18. Ronchi F, Sereno A, Paide M, Sacre P, Guillaume G, Stephenne V, et al. Development and evaluation of an omeprazole-based delayed-release liquid oral dosage form. Int J Pharm. 2019;567:118416.
19. Rhodes CT, Porter SC. Coatings for controlled-release drug delivery systems. Drug Dev Ind Pharm. 1998;24:1139-54.

20. Thakral S, Thakral NK, Majumdar DK. Eudragit®: a technology evaluation. Expert Opin Drug Deliv. 2013;10:131-49.
21. Dos Santos J, Da Silva GS, Velho MC, Beck RCR. Eudragit®: a versatile family of polymers for hot melt extrusion and 3D printing processes in pharmaceutics. Pharmaceutics. 2021;13:1424.
22. Dallas P. Handbook of Laboratory Exercises for the Undergraduate Pharmacy Students in National and Kapodistrian University of Athens. Athens: National and Kapodistrian University of Athens; 2023.
23. Brockmeier D, Voegele D, Von Hattingberg H. In vitro-in vivo correlation, a time scaling problem? Basic techniques for testing equivalence. Arzneimittelforschung. 1983;33:598-601.
24. Moore JW, Flanner HH. Mathematical comparison of dissolution profiles. Pharm Technol. 1996;20:64-74.
25. United States Pharmacopeia and National Formulary (USP 29-NF24). Rockville (MD): United States Pharmacopeial Convention; 2005.
26. Ruiz MA, Reyes I, Parera A, Gallardo V. Determination of the stability of omeprazole by means of differential scanning calorimetry. J Therm Anal Calorim. 1998;51:29-35.
27. Markovic N, Agotonovic-Kustrin S, Glass B, Prestidge CA. Physical and thermal characterisation of chiral omeprazole sodium salts. J Pharm Biomed Anal. 2006;42:25-31.
28. Murakami FS, Lang KL, Mendes C, Cruz AP, Carvalho-Filho MA, Silva MA. Physico-chemical solid-state characterization of omeprazole sodium: thermal, spectroscopic and crystallinity studies. J Pharm Biomed Anal. 2009;49:72-80.
29. Yohana Chaerunisaa A, Sriwidodo, Abdassah M. Microcrystalline cellulose as pharmaceutical excipient. In: Ahmad U, Akhtar J, editors. Pharmaceutical Formulation Design—Recent Practices. London: IntechOpen; 2020.
30. Vlachou M, Pippa N, Siamidi A, Kyrili A. Thermal analysis studies on the compatibility of furosemide with solid state and liquid crystalline excipients. Hem Ind. 2020;74:15-23.
31. Soares JP, Santos JE, Chierice GO, Cavalheiro ETG. Thermal behavior of alginic acid and its sodium salt. Eclet Quim. 2004;29:57-63.
32. Chadha R, Bhandari S. Drug-excipient compatibility screening: role of thermoanalytical and spectroscopic techniques. J Pharm Biomed Anal. 2014;87:82-97.
33. Chen T, Li J, Chen T, Sun CC, Zheng Y. Tablets of multi-unit pellet system for controlled drug delivery. J Control Release. 2017;262:222-31.
34. Murthy Dwibhashyam VS, Ratna JV. Key formulation variables in tableting of coated pellets. Indian J Pharm Sci. 2008;70:555-64.
35. Türkoğlu M, Varol H, Çelikok M. Tableting and stability evaluation of enteric-coated omeprazole pellets. Eur J Pharm Biopharm. 2004;57:279-86.
36. Tan X, Hu J. Investigation for the quality factors on the tablets containing medicated pellets. Saudi Pharm J. 2016;24:507-14.
37. Bodmeier R. Tableting of coated pellets. Eur J Pharm Biopharm. 1997;43:1-8.
38. Efentakis M, Buckton G. The effect of erosion and swelling on the dissolution of theophylline from low and high viscosity sodium alginate matrices. Pharm Dev Technol. 2002;7:69-77.
39. Holte Ø, Onsøyen E, Myrvold R, Karlsen J. Sustained release of water-soluble drug from directly compressed alginate tablets. Eur J Pharm Sci. 2003;20:403-7.
40. Ghahramanpoor MK, Najafabadi SAH, Abdouss M, Bagheri F, Eslaminejad MB. A hydrophobically-modified alginate gel system: utility in the repair of articular cartilage defects. J Mater Sci Mater Med. 2011;22:2365-75.
41. Draget KI, Skjåk-Bræek G, Smidsrød O. Alginate based new materials. Int J Biol Macromol. 1997;21:47-55.
42. Liew CV, Chan LW, Ching AL, Heng PWS. Evaluation of sodium alginate as drug release modifier in matrix tablets. Int J Pharm. 2006;309:25-37.
43. Enobakhare B, Bader DL, Lee DA. Concentration and M/G ratio influence the physiochemical and mechanical properties of alginate constructs for tissue engineering. J Appl Biomater Biomech. 2006;4:87-96.
44. Martinsen A, Storrø I, Skjåk-Bræk G. Alginate as immobilization material: III. Diffusion properties. Biotechnol Bioeng. 1992;39:186-94.
45. Yamagiwa K, Kozawa T, Ohkawa A. Effects of alginate composition and gelling conditions on diffusional and mechanical properties of calcium alginate gel beads. J Chem Eng Jpn. 1995;28:462-7.

46. Rowe RC, Sheskey PJ, Quinn ME. Handbook of Pharmaceutical Excipients. 6th ed. London: RPS Publishing; 2009.
47. Vlachou M, Tsiakoulia A, Eikosipentaki A. Controlled release of the pineal hormone melatonin from hydroxypropylmethylcellulose/sodium alginate matrices in aqueous media containing dioctyl sulfosuccinate. Curr Drug Discov Technol. 2007;4:31-8.
48. Narang AS, Desai D, Badawy S. Impact of excipient interactions on solid dosage form stability. Pharm Res. 2012;29:2660-83.
49. Franco P, De Marco I. The use of poly(N-vinyl pyrrolidone) in the delivery of drugs: a review. Polymers (Basel). 2020;12:1114.
50. Mandal S, Basu SK, Sa B. Sustained release of a water-soluble drug from alginate matrix tablets prepared by wet granulation method. AAPS PharmSciTech. 2009;10:1348-56.
51. Patra CHN, Pandit HK, Singh SP, Devi MV. Applicability and comparative evaluation of wet granulation and direct compression technology to Rauwolfia serpentina root powder: a technical note. AAPS PharmSciTech. 2008;9:100-4.
52. Reza MMM, Bhuiyan MA, Quadir MA. Comparative evaluation of wet granulation and direct compression methods for preparation of compressed tablets using Avicel PH 101. Bangladesh Pharm J. 2002;12:19-22.
53. Park JH, Kwon DY, Heo JY, Park SH, Park JY, Lee B, et al. Effect of drug carrier melting points on drug release of dexamethasone-loaded microspheres. Tissue Eng Regen Med. 2017;14:743-53.
54. Park JH, Kang HJ, Kwon DY, Lee BK, Lee B, Jang JW, et al. Biodegradable poly(lactide-co-glycolide-co-ε-caprolactone) block copolymers: evaluation as drug carriers for a localized and sustained delivery system. J Mater Chem B. 2015;3:8143-53.
55. Park JH, Lee BK, Park SH, Kim MG, Lee JW, Lee HY, et al. Preparation of biodegradable and elastic poly(ε-caprolactone-co-lactide) copolymers and evaluation as a localized and sustained drug delivery carrier. Int J Mol Sci. 2017;18:671.